RSC Advances

ROYAL SOCIETY OF CHEMISTRY

www.rsc.org/advances

Application of Modified Chitosan Microspheres for Nitrate and Phosphate Adsorption from Aqueous Solution

Tingting Zhao, Tao Feng*

College of Resources and Environmental Engineering, Wuhan University of Science and Technology, Wuhan 430081 China

***Corresponding author:** Tel/Fax: +86 27 68862877

E-mail address: fengtaowhu@163.com

Contract grant sponsor: National Natural Science Foundational of China (50904047); Hubei Provincial Department of Education (D20141106).

Abstract:

The modified chitosan microspheres (CM) were prepared by inverse suspension crosslinking and characterized by Fourier transform infrared spectrophotometer, scanning electron microscope and X-ray diffraction. A systematic study of the adsorption of nitrate and phosphate on CM was performed by varying pH, the initial concentration, contact time, and adsorbent dosage. The experimental results showed that CM is an excellent adsorbent for the removal of nitrate and phosphate with an adsorption capacity of 32.15 mg g^{-1} and 33.90 mg g^{-1}, respectively. Equilibrium isotherms study showed a very good fit with the Langmuir isotherm equation for the monolayer adsorption process. Kinetics parameters of the adsorption process indicated that it followed the pseudo-second order equation。

Key words: Chitosan; Microspheres Adsorption; Nitrate; Phosphate

1. Introduction

Nitrate and phosphate are necessary nutrients for biological organisms; however, they may become water contamination if they exceed the limit. Those excess nutrients stimulate eutrophication in water bodies, which indirectly affects human beings though food chain[1]. Methemoglobinemia is a major health problem in infants as well as stomach cancer in adults due to the higher concentration of nitrate in drinking water[2]. Thus, there is obviously a need for the removal of these excess nutrients from water.

A variety of common methods have been investigated for the removal of dissolved nutrients in water and wastewaters such as biological method[3],

ion-exchange[4], absorption method[5], chemical precipitation[6], electro coagulation[7,8] and membrane process[9,10]. Among them, absorption methods are regarded as the most promising technologies because of their low cost, ease of equipment use and lower sludge production[11]. Therefore, the production of ecofriendly polymeric materials is a good choice for the removal of nitrate and phosphate.

In recent years, chitosan (CS) have been given much attention because they are environment-friendly and low-cost biosorbents[12]. Chitosan, a biopolymer having both amino and hydroxyl groups in its skeleton, is the deacetylated product of chitin, consist of 2-acetoamide-2-deoxy-b-D-glucose and 2-amino-2-deoxy-b-D-glucose in various proportions connected through (1→4)-glucoside linkages[13]. The existence of hydroxyl and amine functional groups shows the good adsorption properties of chitosan for many ions[14], especially for the removal of various heavy metal ions and dyes. However, the only drawback of pure chitosan is its poor mechanical strength, which can be easily dissolved in acid media [15], but it is lucratively improved using cross-linking process. In order to overcome the weakness, cross-linking agents such as glutaraldehyde, epichlorohydrin and ethylene glycol diglycidyl ether are usually used to make chitosan chemically and mechanically stable[16].

The reports about the adsorption of nitrate and phosphate using modified chitosan as an adsorbent are very scarce. This study was carried out with an intention to prepare a novel type of modified chitosan microspheres by incorporating formaldehyde, PEG, and epichlorohydrin (ECH), and the adsorption capacity of CM on the removal of nitrate and phosphate was studied using batch studies. The effects

of pH, initial concentration, contact time, and dosage on the adsorption were investigated in detail. The adsorption kinetics and isotherms for nitrate and phosphate onto CM were also studied.

2. Materials and methods

2.1 Reagents and instruments

Chitosan with its deacetylation degree of 90% was supplied by Zhejiang Ocean Biochemical Company. Analytical grade $NaNO_3$ and KH_2PO_4 were used as the source of nitrate and phosphate anions, respectively. NaOH, HCl, PEG_{2000} (which was used as the porogen), Span-80, liquid paraffin, glacial acetic acid, formaldehyde and epichlorohydrin were also of analytical grade. Distilled water was used throughout the study.

T6-new-century ultraviolet absorption spectrophotometer (Beijing PERSEE spectral instrument Co., LTD. Provide), HY-6 double multi-purpose speed oscillator (Jiangsu Jintan Ronghua instrument manufacture Co., LTD. Provide), ISC-90 (Dionex Co., USA, Provide).

2.2 Preparation of CM

In a 2% (v/v) aqueous acetic acid solution, 4 g pure chitosan was dissolved to prepare a 5% (v/v) chitosan solution, and in the same way, 2g PEG_{2000} was dissolved to prepare a 2% (v/v) PEG solution. Poured the PEG solution into chitosan solution, and 100mL liquid paraffin and a certain amount of Span-80 were added to the mixture. The mixed liquor was stirred violently at 313.15 K for 1h until it emulsified, then

added in 30mL formaldehyde and stirred for 2h. Poured the mixture into a large amount of anhydrous alcohol/10% NaOH (v:v=1:1) mixture, and then abandoned the upper water and oil. Pre-crosslinked microspheres were prepared after washing and vacuum filtering repeatedly. The wet microspheres were immersed in a certain amount of 0.1% (v/v) ECH solution at 343.15K for 4h. Afterwards, the wet microspheres were rinsed with distilled water to remove unreacted ECH. The wet microspheres were kept in 0.5mol L^{-1} hydrochloric acid solution overnight and latter soaked with 5% sodium hydroxide solution for several hours. Finally, the modified chitosan microspheres were washed repeatedly with distilled water until it became neutral and dried in vacuum condition. The schematic of reaction principle was showed in Fig.1.

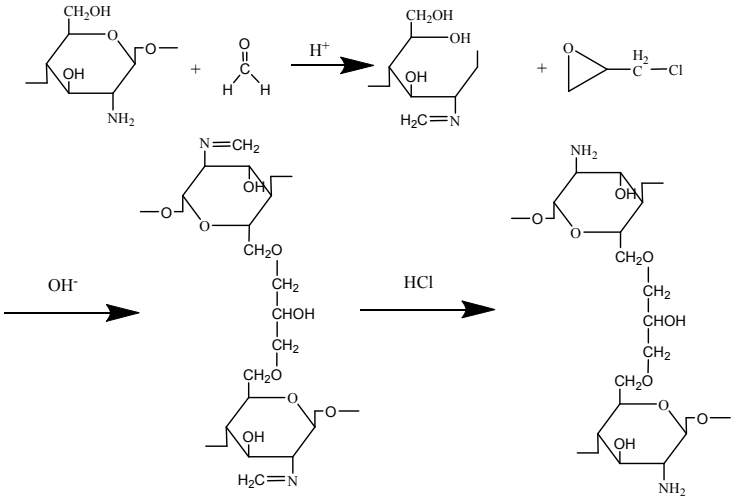

Fig.1 The schematic of reaction principle

2.3 Characterization of CM

The samples formed into pellets with KBr at the ratio of 1:100 (w/w). FTIR spectra were recorded with KBr pellets on Nicolet-360 FT-IR spectrometer over the wave range of 4000-400cm^{-1}.

The SEM analysis was performed to understand the morphology of the samples. Before the observation of SEM, all the samples were fixed on the conductive adhesive and plated with gold. Then they were taken by Nova 400 Nano SEM.

The crystal structure of the samples was investigated by means of XRD method.

2.4 Batch absorption studies

Batch absorption studies were carried out in stopper conical flasks containing 50mL of nitrate or phosphate solution and a certain amount of modified chitosan microspheres. Then the mixture was agitated in double multi-purpose speed oscillator (120 rpm, 303.15K) for desired time followed by filtration. The left out phosphorus content and nitrate content in the supernatant solution after adsorption process was analyzed immediately by using ammonium molybdate spectrophotometric method[17] at a wavelength of 700 nm and ion chromatography method[18] respectively. The adsorption capacity of CM is calculated from the following equation (mg g^{-1})**:**

$$Q=\frac{(C_0-C)V}{1000m} \quad (1)$$

Where C_0, C, respectively, represent the concentration (mg L^{-1}) of nitrate or phosphate in solution before and after adsorption, V is the volume of reaction solution (50mL), m is the quality (g) of dry microspheres.

3. Results and discussion

3.1 Characterization of the materials

3.1.1 FTIR spectra of CS

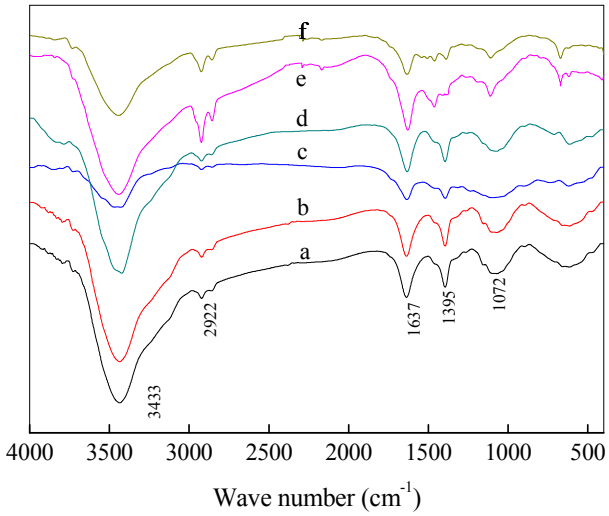

Fig.2 FTIR spectra of CS: pure chitosan (a), chitosan crossed-linked by formaldehyde (b), chitosan crossed-linked by formaldehyde and epichlorohydrin without treating by HCl (c), CM (d), nitrate adsorbed CM (e) and phosphate adsorbed CM(f).

Fig.2 shows the FTIR spectra of pure chitosan, pre-crosslinked microspheres, cross-linked microspheres, CM, nitrate/phosphate adsorbed CM. For pure chitosan (a), the predominant peaks at 3433 cm^{-1}, 2922 cm^{-1}, 1637 cm^{-1}, 1395 cm^{-1} and 1072 cm^{-1} are indicative of -OH and -NH stretching vibrations, C-H stretching vibrations, -NH bending vibration in $-NH_2$ and -C=O stretching vibrations in acetylamino, -NH deformation vibration in $-NH_2$, and -CO stretching vibration, respectively.

Then the chitosan crossed-linked with formaldehyde (b), the overlapped peaks of $-NH_2$ and -OH became wider, weaker and moved from 3433 cm^{-1} to 3443cm^{-1}. The absorption peaks at 1070 cm^{-1}, 1396 cm^{-1} and 2922 cm^{-1} decreased obviously. All of them indicated that $-NH_2$ and -OH involved the cross-link process. In addition, the absorption peaks at 1637 cm^{-1} became wider and stronger, which accounted for the formation of shiff base and protect the amino group.

After the microspheres cross-linked by ECH (c), the stretching vibrations peaks

at 3423 cm^{-1} almost disappeared and the bending vibrations at 1634 cm^{-1} almost unchanged. Furthermore, the -CO stretching vibrations became weaker. Therefore, -OH had participated in cross-link process.

After the microspheres treated by HCl (d) finally, the $–NH_2$ stretching vibrations and bending vibrations became stronger, and the peaks of shiff base at 1632 cm^{-1} was covered by the peaks of $-NH_2$, indicating that most of the shiff base can be removed by hydrochloric acid treatment.

As showed in Fig.2, sharp peak at 1395 cm^{-1} in the nitrate adsorbed CM was contributed by N-O stretching. At 1072 cm^{-1} a slight broadening was there in the phosphate adsorbed CM due to the presence of phosphate. While the infrared spectrum of nitrate/phosphate adsorbed CM has little change compared to the CM, indicating that the adsorption process is closer to physical adsorption.

3.1.2 Morphology of CM

SEM micrographs of pure chitosan microspheres (a) and CM (b) are shown in Fig.3. It was evident that the surfaces of pure chitosan microspheres were relatively flat, homogeneous and smooth. However, the surfaces of CM were roughness and the porous microstructure showed clearly. The presence of porous surface structure may increas the specific surface area leading a higher degree of adsorption efficiency. According to the SEM images in Fig.3, the adsorbent particles were micronsized and spheroidal, and the sizes were about 100 μm.

3.1.3 XRD analysis

Fig.3(c) shows the XRD pattern of CS and CM. As shown, the pure chitosan has

strong diffraction peaks at 2θ=12.71°and 20.16°, after cross-linked by formaldehyde and ECH, the characteristics of diffraction peak at 12.71°almost disappeared, and the diffraction peaks of CM became obviously weaker and shifted to 21.03°. At the same time, the amorphous area increased apparently at 21.03°.These changes indicated that the crystallinity of CM decreased compared with the CS.

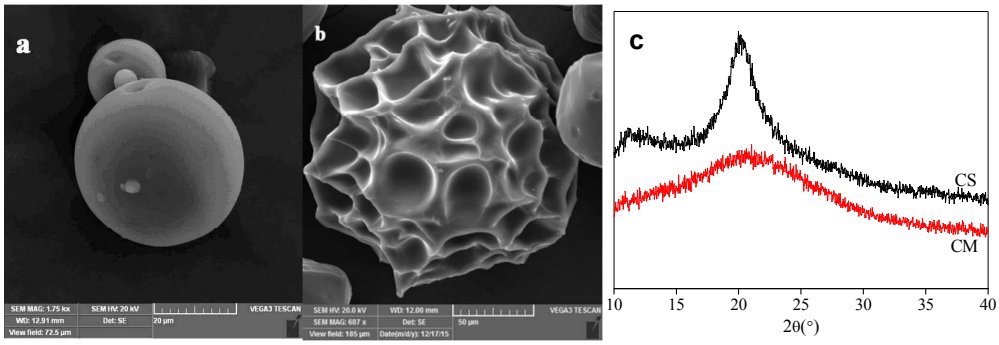

Fig.3 SEM micrographs of pure chitosan microspheres (a) and CM (b), and the XRD spectra of chitosan microspheres(c)

3.2 Factors that affect the anion adsorption

3.2.1 Effect of pH on adsorption capacity

The pH is the most important factor affecting the adsorption process. To investigate the effect of pH on the adsorption performance, the initial pH values was adjusted to 2.0-9.0 by 0.1 mol L^{-1} HCl or 0.1 mol L^{-1} NaOH solutions. The initial concentration of the phosphate aqueous solution and nitrate aqueous solutions was 10.0mg L^{-1} and 20.0mg L^{-1}, respectively. 0.05g CM were weighted and added into the solutions at different pH values under oscillating at 303.15K for 3h. Fig.4 showed the *Q* of CM at different pH of initial solution. It can be observed that the adsorption capacity changed dramatically in pH of the initial solution from 2.0 to 4.0, and decreased gradually thereafter. The maximum absorption capacity reached at pH 3.0, and the adsorption capacity of phosphate and nitrate was 8.69 mg g^{-1} and 13.51mg g^{-1},

respectively.

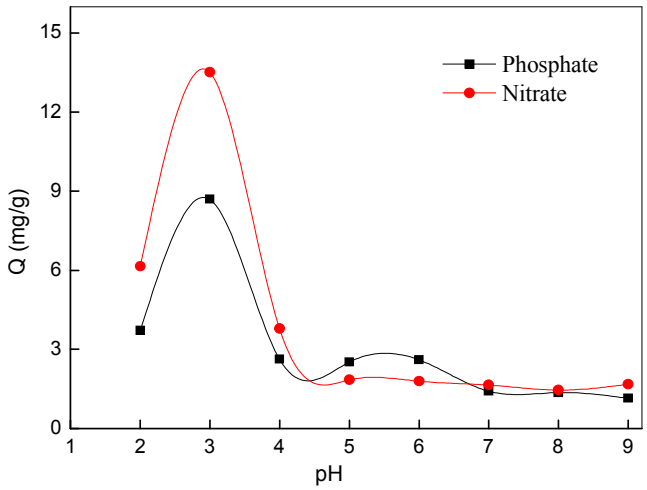

Fig.4 Effect of pH on adsorption capacity

The surface charge of the adsorbent and the ionization degree of the adsorbate are strongly affected by the pH of the aqueous solutions[19]. The $–NH_2$ of chitosan can be combined with H^+, and exist the following balance:

$$H^+ + RNH_2 \leftrightharpoons RNH_3^+$$

So there seems to be a significant impact on the ionization ability of $-NH_2$ by pH, which affects the adsorption capacity of target ions. There are a lot of H^+ in solution when pH is low, $-NH_2$ of chitosan are protonated in this environment. This behavior will enhance the electrostatic attraction of anions, further increasing the adsorption capacity of target ions. But at pH 2.0, the adsorption capacity decreased, which may relate to the stability of modified chitosan in strong acid solution: the chitosan will degrade due to the large number of H^+, resulting in chain scission macromolecule, reduction in molecular weight[20]. As the amino cannot ionization in alkaline, the adsorbent can only rely on the surface energy of itself to the target ions sorption. Besides that, with the rise of pH, more and more hydroxyl ions compete with the

target ions, which hence the decrease in the adsorption capacity[21]. As is known to us all, phosphate can exist in the form of H_3PO_4, $H_2PO_4^-$, HPO_4^{2-} and PO_4^{3-}, respectively, at pH ranges of <2.0, 2.0-7.0, 7.0-12.5 and >12.5[22]. The results illustrate that phosphate adsorbed well on CM irrespective of $H_2PO_4^-$.

3.2.2 Effect of initial nitrate and phosphate concentration on adsorption capacity

The effect of initial solution concentration on the removal of nitrate and phosphate were carried out by vibrating 50mL various concentration of phosphate aqueous solution and nitrate aqueous solution at pH 3.0 and adding 0.05 g CM under oscillating at 303.15K for 3h. Fig.5 showed that the *Q* of phosphate increased from 8.69 to 31.45mg g^{-1} with the increase in initial PO_4^{3-}-P concentration from 10 to 100mg L^{-1}, while the *Q* of nitrate increased slowly from 7.03 to 28.49mg g^{-1} with the increase in initial NO_3^- concentration from 10 to 100 mg L^{-1}. The results illustrate that higher concentration gradient acting as a driving force overcame mass transfer resistance between bulk solution and adsorbent surface[23].

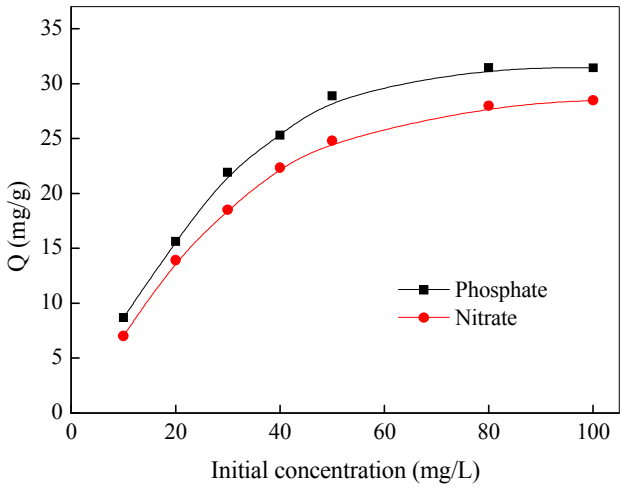

Fig.5 Effect of initial concentration on adsorption capacity

3.2.3 Effect of contact time on adsorption capacity

Contact time studies are helpful in understanding the amount of ions adsorbed at various time intervals by a fixed amount of the adsorbent. To investigate the effect of contact time on adsorption of nitrate and phosphate, 10mg L^{-1} of PO_4^{3-}-P solutions and 20mg L^{-1} of nitrate solutions at pH 3.0 under 303.15K were contacted with 1g L^{-1} of CM, respectively. The samples were taken out at different periods of time and analyzed for the left out concentration.

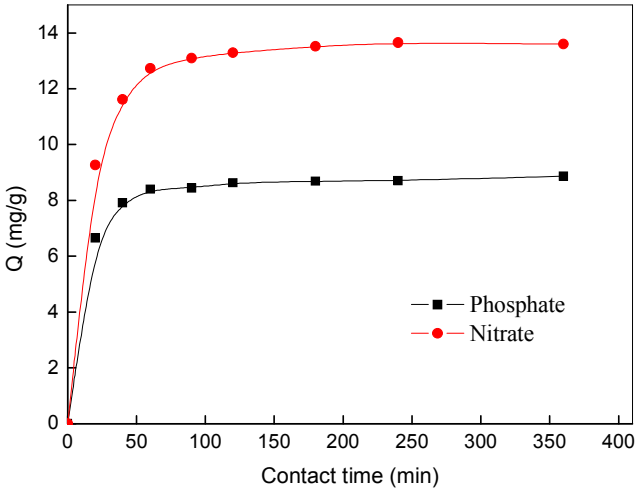

Fig.6 Effect of contract time on adsorption capacity

The result was shown in Fig.6. It clearly indicates that the adsorption capacity of nitrate and phosphate onto CM increases rapidly within 40 min and then slows down gradually until it attains equilibrium. It would be for that a large number of vacant surface sites are available for adsorption during the initial stage of the treatment time, and after a lapse of time, the remaining vacant surface sites are difficult to be occupied due to repulsive forces between nitrate/phosphate adsorbed on the surface of CM and solution phase. Under our experimental conditions, the equilibrium time for

the adsorption of nitrate and phosphate onto CM was 90 min. The maximal nitrate and phosphate uptake by CM was 13.93 mg g^{-1} and 8.87 mg g^{-1}, respectively.

3.2.4 Effect of adsorbent dosage capacity

Adsorbent dosage was also a vital parameter influencing adsorption capacity, therefore, absorption experiments were carried out with initial solution concentration at pH 3.0. Different doses of the CM powder were weighted and added to solutions under oscillating at 303.15K for 3h. The effect of adsorbent dosage on nitrate and phosphate removal was depicted in Fig.7. It was evident that the adsorption capacity of nitrate on CM decreased from 21.90 to 6.77 mg g^{-1}, but the removal rate increased from 21.9% to 71.18% with the increase in adsorbent dosage from 0.2 to 2g L^{-1}. At the same time, the adsorption capacity of phosphate decreased from 26.45 to 4.58 mg g^{-1} with the increase in adsorbent dosage while the removal rate increased from 52.89% to 91.64%. The result indicated that with an increase in adsorbent dose, the number of active sites increased[24], the uptakes of target ions increased till a certain value and thereafter remains nearly constant. As shown in Fig.7, the removal percentage was little changed when the adsorbent dosage was greater than 1 g L^{-1}. Therefore, it is suggested that the effectiveness decreased with an increase of adsorbent dosage beyond 1 g L^{-1}. Above all, 1 g L^{-1} can be regarded as the optimal dosage.

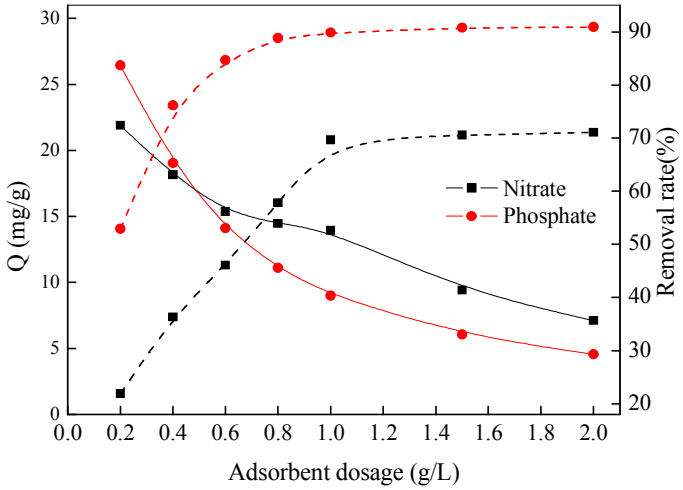

Fig.7 Effect of adsorbent dosage on adsorption capacity (the solid line) and removal rate (the dash line)

3.3 Kinetic studies

In order to investigate the mechanism of the sorption and describe the adsorption rate of the absorbents, the pseudo-first-order, pseudo-second-order rate models and intraparticle diffusion models were used in this study.

A kinetic model for sorption analysis is the first-order rate expression of Lagergren[25] in the form:

$$\frac{dQ_t}{dt}=k_1 t(Q_e-Q_t) \quad (2)$$

Where Q_e (mg g^{-1}) and Q_t (mg g^{-1}) denote the amounts adsorbed at equilibrium and at any time t, respectively, and k_1 (min^{-1}) is the rate constant of first-order sorption.

The rearranged form of Eq. (2) is

$$\ln(Q_e-Q_t)=\ln Q_e-k_1 t \quad (3)$$

The pseudo-second-order kinetic model[26] is expressed as

$$\frac{t}{Q_t}=\frac{1}{k_2 Q_e^2}+\frac{1}{Q_e}t \quad (4)$$

Where Q_e (mg g^{-1}) and Q_t (mg g^{-1}) denote the amounts adsorbed at equilibrium and at any time t, respectively, and k_2 (g $min^{-1}mg^{-1}$) is the rate constant of second-order sorption.

The intraparticle diffusion models was firstly proposed by Weber[27], and the equation is

$$Q_t=k_p t^{1/2}+C \quad (5)$$

Where Q_t (mg g^{-1}) denotes the amounts adsorbed any time t, and k_p is the intraparticle diffusion rate constant.

The fitting figures of pseudo first-order, second-order models and intraparticle diffusion models are shown in Fig.8, respectively, and the calculated parameters are given in Table 1. The correlation coefficient R^2 for the pseudo first-order, second-order models are both higher than 0.95. It's obvious that both models can describe the adsorption kinetics of nitrate onto CM very well, which indicated that the adsorption behaviors were mainly ascribed to both physic-sorption and chemic-sorption. Based on the correlation coefficient R^2 values, it could be seen that the pseudo-second-order mechanism rather than the pseudo-first-order mechanism conforms to the phosphate adsorption processes, which indicates that chemisorptions might be the rate-limiting step that controls these adsorption processes. As the Fig.8(c) shows, the adsorption process was divided into two phases, including a fast adsorption phase on the surface of the adsorbent and a slow pore diffusion phase. In addition, we can see the fitted curves didn't pass through the origin point, which indicates that the

intraparticle diffusion is not the only limiting step during the adsorption process.

Table 1 Adsorption parameters of kinetic for the adsorption of nitrate and phosphate on CM.

Ions	Pseudo-first-order kinetic models			Pseudo-second-order kinetic models		
	Q_e (mg g^{-1})	k_1 (min^{-1})	R^2	Q_e (mg g^{-1})	k_2 (g $min^{-1}mg^{-1}$)	R^2
Nitrate	5.117	0.0209	0.9830	14.045	0.0093	0.9998
Phosphate	1.552	0.0125	0.9523	9.001	0.0194	0.9999
Ions	Intraparticle diffusion models					
	kp_1 (g $min^{-1}mg^{-1}$)	C_1	R^2	kp_2 (g $min^{-1}mg^{-1}$)	C_2	R^2
Nitrate	1.0684	4.6013	0.9683	0.0833	12.27	0.8286
Phosphate	0.5434	4.2950	0.9389	0.0432	8.091	0.9078

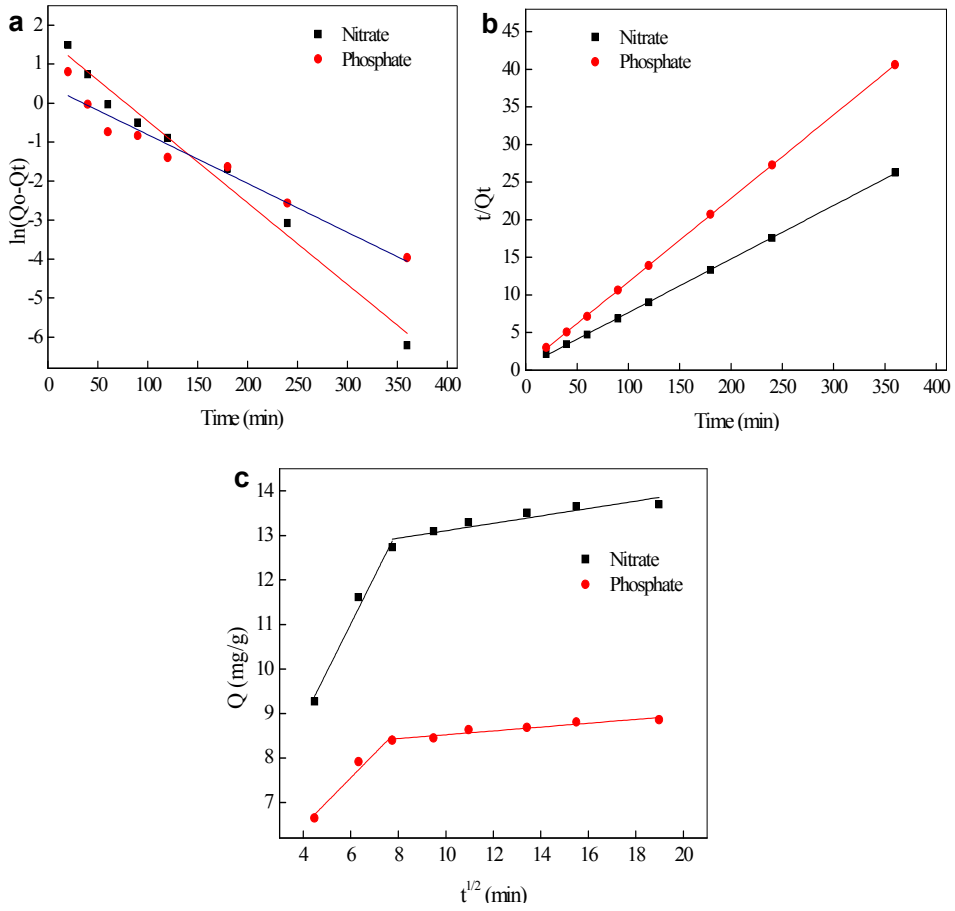

Fig.8 Pseudo first-order (a), second-order (b) kinetics and intraparticle diffusion(c) models for nitrate and phosphate sorption on CM

3.4 Adsorption isotherm

In order to evaluate the relationship between the amount of nitrate and phosphate sorbed by CM at a constant temperature and its equilibrium concentration in aqueous solution, Langmuir[28], Freundlich[29,30] and Dubinin-Radushkevich[31] isotherm models were used in the study.

The Langmuir model assumes that adsorption takes place at specific homogeneous sites on the surface of adsorbent and also, when a site is occupied by an adsorbate molecule, no further adsorption can take place at this site. The Langmuir isotherm model can be presented as:

$$Q_e = \frac{Q_{max} b C_e}{1 + b C_e} \quad (6)$$

Where Q_e, Q_{max} (mg g^{-1}), respectively, represent the equilibrium and maximum adsorption capacity, C_e (mg L^{-1}) is the equilibrium concentration of nitrate and phosphate in the aqueous solution, b is the Langmuir constant related to the affinity of the binding sites.

The linear form of Eq. (6) is

$$\frac{C_e}{Q_e} = \frac{C_e}{Q_{max}} + \frac{1}{Q_{max} b} \quad (7)$$

The Freundlich equation is purely empirical based on sorption on heterogeneous surface and is given by:

$$Q_e = k C_e^{1/n} + C \quad (8)$$

Where k is the Freundlich constant related to the adsorption capacity, $1/n$ is the Freundlich constant related to the adsorption intensity, C is the constant.

The rearranged form of Eq. (8) is

$$\log Q_e = \log k + 1/n \log C_e \quad (9)$$

Dubinin–Radushkevich isotherm assumes that the characteristic sorption curve is related to the porous structure of the sorbent and apparent energy of adsorption[32]. This model is given by

$$Q_e = Q_{max} \exp(-Be^2) \quad (10)$$

$$E = 1/\sqrt{(2B)} \quad (11)$$

Where B ($mol^2\ kJ^{-2}$) is a constant related to the free energy, e is the Polanyi potential, equal to $RT\ln(1+1/Ce)$ and E ($kJ\ mol^{-1}$) is the average adsorption energy. The linearized form is

$$\ln Q_e = \ln Q_{max} - 2BRT\ln(1+1/C_e) \quad (12)$$

Where R is the ideal gas constant, 8.314 $J\ mol^{-1}\ K^{-1}$, T (K) is the thermodynamic temperature.

The corresponding information was shown in Fig.9 and Table 2. Table 2 shows the calculated values of Langmuir, Freundlich and Dubinin-Radushkevich models' parameters at different temperatures. It is obvious that the maximum adsorption capacity (Q_{max}) of CM decreased with the increasing temperature, which indicated that the temperature has a certain effect on the adsorption. The correlation coefficient R^2 of Langmuir and Freundlich isothermal model for nitrate and phosphate sorption had high values, indicating that both two well-known isotherms are suitable for describing the equilibrium data. From Table 2, it can be seen that the R^2 of Langmuir isotherm is higher than that of Freundlich isotherm, which showed that the nitrate and phosphate anions are mainly adsorbed in monolayer coverage manner without

interaction amidst the adsorbed ions[30]. It is hence considered the values of Q_{max} deduced from the Langmuir model could reflect the adsorption ability of the composite. From the Langmuir models, the maximum adsorption capacity at 303.15K of CM for nitrate was 32.15 mg g^{-1}, while Q_{max} for phosphate was 33.90 mg g^{-1}. From Table 2, the value of 1/*n* is between 0.1 and 0.5, indicating the easy uptake of ions from aqueous solution. It's clear that the value of 1/*n* for phosphate is lower than the one for nitrate, indicating a higher affinity for phosphate adsorption. In addition, the Langmuir isothermal model can be commendably instead of Dubinin-Radushkevich isothermal model. Although the theoretical values of R^2 and Q_{max} are relatively lower compared to the Langmuir models, yet they are also close to the experimental data. The calculated values of *E* from the Dubinin-Radushkevich isotherm give information about the chemical or physical properties of the sorption. If the magnitude of *E* is between 8 and 16 kJ mol^{-1}, the adsorption process proceeds by ion exchange, while for values of $E < 8$ kJ mol^{-1}, the adsorption process is of a physical nature[32]. Since the *E* values obtained from Dubinin-Radushkevich isotherm were less than 8 kJ mol^{-1}, which further confirmed the presence of physical adsorption forces.

Table 2 Adsorption parameters of isotherms for the adsorption of nitrate and phosphate on CM.

Ions	Temperature	Langmuir			Freundlich			Dubinin-Radushkevich			
		Q_{max} (mg g^{-1})	b	R^2	1/*n*	*k* (L g^{-1})	R^2	Q_{max} (mg g^{-1})	*B* (mol^2 kJ^{-2})	E (kJ mol^{-1})	R^2
Nitrate	303.15	32.154	0.1147	0.9978	0.4184	5.7214	0.8858	29.705	1.01×10^3	0.0223	0.9939
	313.15	27.397	0.0867	0.9951	0.4292	4.3033	0.9069	23.905	1.13×10^3	0.0210	0.9467
	323.15	25.189	0.0821	0.9480	0.4354	3.8291	0.9015	22.488	1.26×10^3	0.0199	0.9605
Phosphate	303.15	33.898	0.2152	0.9992	0.3957	8.1452	0.9153	31.785	5.82×10^2	0.0293	0.9850
	313.15	25.126	0.1641	0.9990	0.3218	6.6390	0.8362	24.262	8.01×10^2	0.0250	0.0990
	323.15	23.256	0.1450	0.9964	0.3564	5.2735	0.8058	23.139	1.04×10^3	0.0219	0.9834

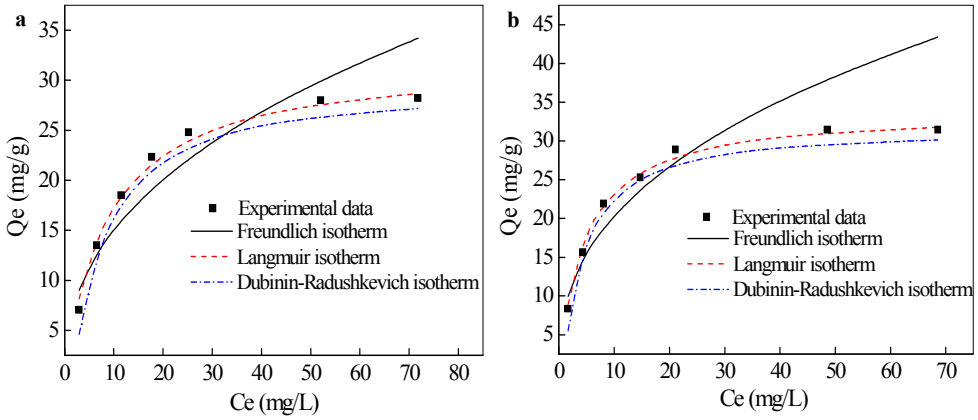

Fig.9 Adsorption isotherms for nitrate (a) and phosphate (b) sorption on CM at 303.15K: Langmuir isotherm (the dash line), Freundlich isotherm (the solid line), Dubinin-Radushkevich isotherm (the dash-dotted line)

Table 3 Comparison of nitrate and phosphate adsorption of CM with adsorbent materials in the references.

Absorbent	pH	Concentration range		Adsorption capacity		References
		Nitrate (mg NO_3^- L^{-1})	Phosphate (mg P L^{-1})	Nitrate (mg NO_3^- L^{-1})	Phosphate (mg P g^{-1})	
CM	3	10-50	10-50	32.15	33.90	This study
$Fe_3O_4/ZrO_2/CS$	3	1-1000	10-300	89.3	26.5	30
Cu(II) -loaded CS	5	-	10-180	-	30.12	33
Graphene	7	-	25-125	-	13.21	32
Polyethylene glycol/Chitosan	3	10-100	-	50.68	-	24
Poly vinyl alcohol/Chitosan	3	10-100	-	35.03	-	24
Ammonium-functionalized MCM-48	4.0-6.0	100-700	100-700	43	14.7	5
Modified Lignite Granular Activated Carbon	5	5-150	-	10.85	-	34
HTDMA modified bentonite	5.4	100	-	14.76	-	35

As far as we know, a number of adsorbents were tested for the removal of nitrate and phosphate from aqueous solution. For comparison, the nitrate and phosphate uptakes by other reported adsorbents are summarized in Table 3. The maximum nitrate and phosphate sorption showed in Table 3 were at pH between 3.0 and 6.0, which indicated that most adsorbents preferred to adsorb dihydrogen phosphate. Among those adsorbents, the adsorption of nitrate on CM was relatively high and the

phosphate uptake of CM was the highest, which indicated that CM has a good adsorptive property. As a natural polymer with lots of hydroxyl and amine functional groups, many ions can be absorbed by chitosan. Furthermore, chitosan has several excellent properties, such as environment-friendly, biocompatibility, security, and microbial degradation. However, it is difficult to be directly used in water treatment due to some inherent shortcomings. Therefore, the crosslink modified chitosan can overcome some shortcomings: the solubility properties of chitosan were improved, and then the range of application was enlarged. In a word, the result all indicated that CM was a promising adsorbent for the removal of both nitrate and phosphate from aqueous solution.

3.5 The regenerative adsorption property of CM

Reusability is another important parameter to evaluate an adsorbent. In the present study, 0.1 mol L^{-1} NaOH solution is used to treat CM which has adsorbed target anions for the removal of the adsorbed ions. The mixture was agitated in double multi-purpose speed oscillator (120 rpm, 303.15K) for 24h followed by filtration, and the wet adsorbents were washed repeatedly with distilled water until it became neutral and dried in vacuum condition. After that, they were used to re-adsorb the target anions. Repeat the experiment 4 times, and the changes of its adsorption capacity are shown in Fig.10. With the increase in the number of regeneration, the adsorption capacity of nitrate and phosphate decreases from 8.10 to 4.78 mg g^{-1} and 6.89 to 4.51 mg g^{-1}, respectively. The result indicates that there could be physical forces besides electrostatic interaction during adsorption course, so the saturated adsorbent cannot be

thoroughly regenerated by strong alkali condition[30].

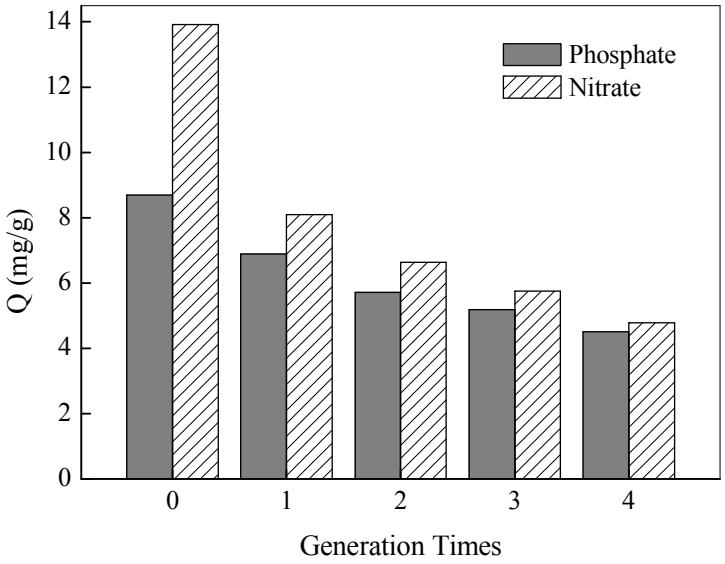

Fig.10 Effect of Generation Times on adsorption capacity

4. Conclusions

The modified chitosan microspheres had a laudable performance for nitrate and phosphate adsorption. The maximum adsorption capacity nitrate and phosphate was 32.15 mg g^{-1} and 33.90 mg g^{-1} based on Langmuir isotherm model. The results demonstrate that the adsorption process is dependent on pH, initial solution concentration, contract time and adsorbent dosage. Langmuir isotherm was the most suitable adsorption isotherm for nitrate and phosphate sorption, and pseudo-second-order kinetic model was the most suitable kinetic model for the adsorption of nitrate and phosphate on CM. Dubinin-Radushkevich isotherm confirmed the presence of physical adsorption forces. From a practical point of view, the CM is promising for treating water that is contaminated with nitrate and phosphate.

Reference

1 M. N. Almasri，J. J and Kaluarachchi ，*J. Hydrol.*，2004，**295**，225-245.

2 Y. W. Lee，M. F. Dahab and I. Bogardi，*J . Water Res. Pl-ASCE.*，1992，**118**(2)，151-165.

3 J. P. Bassin，R. Kleerebezem，M. Dezotti and M. C. M. V. Loosdrecht，*Water Res.*，2012，**46**(12)，3805-3816.

4 X. Xu，B. Y. Gao，Q. Y. Yue and Q. Q. Zhong，*Bioresource Technol.*，2010，**101**(22)，8558-8564.

5 R. Saad，K. Belkacemi and S. Hamoudi，*J. Colloid. Interf. Sci.*，2007，**311**(2)，375-381.

6 A. H. Caravelli，C. D. Gregorio and N. E. Zaritzky，*Chem. Eng. J.*，2012，**209**(20)，469-477.

7 E. Lacasa，P. Cañizares，C. Sáez，F. J. Fernández and M. A. Rodrigo，*Chem. Eng. J.*，2011，**171**(3)，1012-1017.

8 S. Vasudevan，J. Lakshmi，J. Jayaraj and G. Sozhan，*J. Hazard. Mater.*，2009， **164**(2-3)，1480-1486.

9 E. J. Mcadam and S. J. Judd，*Desalination*，2006，**196**(s1-3)，135-148.

10 M. M. H. Senna，Y. K. Abdel-Moneam，O. A. Gamal and A. Alarifi，*J. Ind. and Eng. Chem.*，2013，**19**(1)，48-55.

11 A. Sowmya and S. Meenaksh，*Int. J. Biol. Macromol.*, 2014，69(8)，336-343.

12 C. Shen，Y. Shen，Y. Wen，H. Wang and W. Liu，*Water Res.*，2011，

45(16)，5200-5210.

13 K. N. Hong and S. P. Meyers，*J. Agric. Food Chem.*，1989，**37**，580-583.

14 M. N. V. R. Kumar，*React. Funct. Polym.*，2000，**46**(1)，1-27.

15 Z. Zhao，N. Liu，L. Yang，J. Wang，S. Song，D. Nie，X. Yang，J. Hou and A. Wu，*Food Control*，**57**，362-369.

16 W. S. W. Nhag，C. S. Endud and R. Mayanar，*J. Nutr. Health. Aging*，2002，**50**(2)，181-190.

17 G. M. Chen，*China Water & Wastewater*，2006，**22**(2)，85-86.

18 D. C. Siu and A. Henshall，*J. Chromatogr. A*，1998，**804**(1-2)，157-160.

19 H. B. Senturk，D. Oades，A. Gundogdu，C. Duran and M. Soylak，*J. Hazard. Mater.*，2009，**172**(1)，353-362.

20 Y. Guo, J. Xue, Q. Bi and Y. Du. *Chin. J. Environ. Eng.*，2013，**7**(6)，2019-2024.

21 A. Sowmya and S. Meenakshi，*J. Environ. Chem. Eng.*，2013，**1**(4)，906-915.

22 A. Sowmya and S. Meenakshi，*Int. J. Biol. Macromol.*，2014，**64**(2)，224-232.

23 Q. Hu， N. Chen， C. Feng and W. W. Hu，*Appl. Surf. Sci.*，2015，**347**，1-9.

24 A. Rajeswari，A. Amalraj and A. Pius，*J. Water Proc. Eng.*，2016，**9**，123-134.

25 A. Zümriye，*Biochem. Eng. J.*，2001，**7**(1)，79-84.

26 Y. S. Ho and G. Mckay，*Process Biochem.*，1999，**34**(5)，451-465.

27 W. J. Weber and J. C. Morris，*Pergamon Press. Oxford*，1962，231.

28 R. Katal, M. S. Baei, H. T. Rahmati and H. Esfandian, *J. Ind. Eng. Chem.*, 2012, **18**(1), 295-302.

29 X. Song, Y. Pan, Q. Wu, Z. Chen and M. Wei, *Desalination*, 2011, **280**(1-3), 384-390.

30 H. Jiang, P. Chen, S. Luo, X. Tu, Q. Cao and M. Shu, *Appl. Surf. Sci.*, 2013, **284**(10), 942-949.

31 M. M. Dubinin. *Chem. Rev.*, 1960, **60**(60), 235-241.

32 S. Vasudevan and J. Lakshmi. *Rsc. Adv.*, 2012, **2**(12), 5234-5242.

33 J. Dai, H. Yang, Y. Han, Q. Zheng and R. Cheng, *Chem. Eng. J.*, 2011, **166**(3), 970-977.

34 M. A. Khan, Y. Ahn, M. Kumar, W. Lee, B. Min, G. Kim, D. Cho, W. B. Park and B. Jeon, *Sep. Sci. Technol.*, 2011, **46**(16), 2575-2584.

35 Y. Xi, M. Mallavarapu and R. Naidu, *Appl. Clay Sci.*, 2010, **48**(1–2), 92-96.

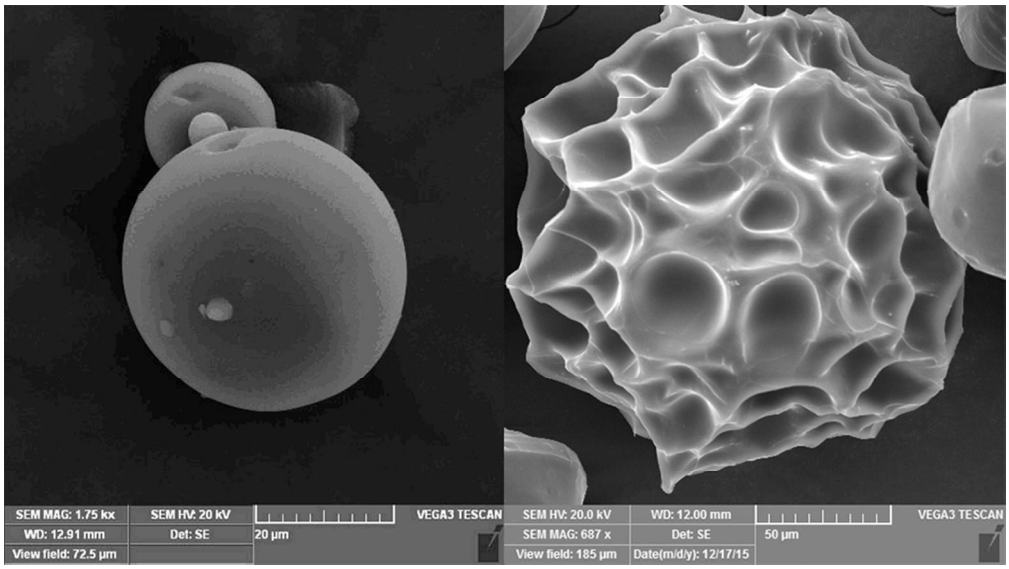

80x44mm (300 x 300 DPI)